Modeling the Acid–Base Properties of Bacterial Surfaces: A Combined Spectroscopic and Potentiometric Study of the Gram-Positive Bacterium Bacillus subtilis

ARTICLE *in* ENVIRONMENTAL SCIENCE AND TECHNOLOGY · OCTOBER 2007

Impact Factor: 5.33 · DOI: 10.1021/es070996e · Source: PubMed

7 AUTHORS, INCLUDING:

Carla Manfredi
University of Naples Federico II
27 PUBLICATIONS **590** CITATIONS
SEE PROFILE

Per Persson
Lund University
144 PUBLICATIONS **4,179** CITATIONS
SEE PROFILE

Andrey Shchukarev
Umeå University
108 PUBLICATIONS **1,396** CITATIONS
SEE PROFILE

Staffan Sjöberg
Umeå University
170 PUBLICATIONS **4,376** CITATIONS
SEE PROFILE

Environ. Sci. Technol. **2007**, *41,* 6465−6471

Modeling the Acid−Base Properties of Bacterial Surfaces: A Combined Spectroscopic and Potentiometric Study of the Gram-Positive Bacterium *Bacillus subtilis*

LAURA LEONE,*,† DIEGO FERRI,‡ CARLA MANFREDI,‡ PER PERSSON,† ANDREI SHCHUKAREV,† STAFFAN SJÖBERG,† AND JOHN LORING†

Department of Chemistry, Umeå University, Umeå, Sweden, and Department of Chemistry, University of Naples "Federico II", Naples, Italy

In this study, macroscopic and spectroscopic data were combined to develop a surface complexation model that describes the acid−base properties of *Bacillus subtilis*. The bacteria were freeze-dried and then resuspended in 0.1 M NaCl ionic medium. Macroscopic measurements included potentiometric acid−base titrations and electrophoretic mobility measurements. In addition, ATR-FTIR spectra of wet pastes from suspensions of *Bacillus subtilis* at different pH values were collected. The least-squares program MAGPIE was used to generate a surface complexation model that takes into account the presence of three acid−base sites on the surface: ≡COOH, ≡NH^+, and ≡PO^-, which were identified previously by XPS measurements. Both potentiometric titration data and ATR-FTIR spectra were used quantitatively, and electrostatic effects at the charged bacterial surface were accounted for using the constant capacitance model. The model was calculated using two different approaches: in the first one XPS data were used to constrain the ratio of the total concentrations of all three surface sites. The capacitance of the double layer, the total buffer capacity, and the deprotonation constants of the ≡NH^+, ≡POH, and ≡COOH species were determined in the fit. A second approach is presented in which the ratio determined by XPS of the total concentrations of ≡NH^+ to ≡PO^- sites is relaxed. The total concentration of ≡PO^- sites was determined in the fit, while the deprotonation constant for ≡POH was manually varied until the minimization led to a model which predicted an isoelectric point that resulted in consistency with electrophoretic mobility data. The model explains well the buffering capacity of *Bacillus subtilis* suspensions in a wide pH range (between pH = 3 and pH = 9) which is of considerable environmental interest. In particular, a similar quantitative use of the IR data opens up possibilities to model other bacterial surfaces at the laboratory scale and help estimate the buffering capacity of carboxylate-containing compounds in natural samples.

Introduction

The chemistry in soils and aquifers is influenced by processes at interfaces between aqueous solutions and natural particles, and for these processes the activity of microbial organisms plays important roles. Bacteria, in particular, are ubiquitous on our planet and constitute a substantial part of the total biomass (10^6−10^9 bacteria per gram of soil) (*1*). Thus, the study of bacterial adsorption properties has received much attention during the last years. It is well-known that bacterial suspensions exhibit acid−base and metal complexing capabilities (*2*, *3*) and that these properties can greatly affect the chemical speciation in natural environments. Since protonation and metal complexation reactions are considered to occur primarily at the interface between the bacterial surfaces and the aqueous solution, then surface complexation modeling approaches can be used to describe these reactions (*4*).

Acid−base surface complexation models proposed previously are based on assumptions about the identities of the functional groups involved in protolytic equilibria on the bacterial surface (*2*, *3*). While these assumptions are reasonable from a macroscopic point of view, they are not based on surface-specific molecular-scale measurements of the bacterial surface. Hence, there is no consensus on a general protonation model.

To further the understanding of protolytic reactions at the water−bacterium interface, spectroscopic studies are necessary to identify the surface functional groups involved in the acid−base reactions and to help determine the conditions under which these groups are proton active. Infrared measurements on Gram-positive and Gram-negative bacteria, and their isolated cell walls, led to the identification of carboxyl, amide, phosphate, hydroxyl groups, and carbohydrate-related moieties on the surface of the cells (*5*). In the work by Yee et al. (*6*), results from IR spectroscopy, potentiometric titrations, and metal adsorption experiments were used to generate both acid−base and metal adsorption models for cyanobacteria. Tentative assignments of the functional groups' identity were made in this study (*6*) by combining information obtained from the IR spectra with the knowledge of cell wall biochemistry, and comparisons with pK_a values of model compounds. However, in this study (*6*) it is also reported that spectral changes related to phosphate groups could not be detected, and deprotonation reactions involving amine and hydroxyl groups were not observed. In the recent publication by Heinrich et al. (*7*) an acid−base Donnan model has been proposed for the Gram-positive bacterium *Anoxybacillus flavithermus*, by using a combined experimental approach which includes IR spectroscopy. In this study (*7*), the presence of carboxylic groups was confirmed by the IR spectra, which also suggested the presence of phosphodiester groups, while the existence of amine groups could not be clearly demonstrated.

Moreover, EXAFS studies have been performed to help elucidate the identity of the functional groups involved in metal binding on *Bacillus subtilis* and other microorganisms. It has been suggested that phosphoryl and carboxylic groups play a major role in the metal complexation reactions (*8*−*10*). However, the existence of other surface sites, such as phosphomonoester, sulfhydryl, amine, and hydroxyl groups, has been proposed elsewhere (*11*).

In this study, we investigate the acid−base reactions at the surface of the Gram-positive bacterium *B. subtilis* in aqueous solution. X-ray photoelectron spectroscopy (XPS) was used to identify the types and ratios of the total

* Corresponding author tel: +46907866072; fax: +46907869195; e-mail: laura.leone@chem.umu.se.
† Umeå University.
‡ University of Naples "Federico II".

10.1021/es070996e CCC: $37.00
Published on Web 08/14/2007

concentrations of the proton-active surface sites. Fourier transform infrared (ATR-FTIR) spectra were collected of wet pastes of the bacteria as a function of pH, and these data reveal changes that are indicative of the protonation of specific sites. Potentiometric titrations were performed to follow the proton uptake at the bacterial surface and electrophoretic mobility measurements were made to investigate the surface charge development as a function of pH. A surface complexation model was generated by using the computer program MAGPIE in which the potentiometric data and the infrared spectra were analyzed simultaneously and quantitatively via a factor analysis. XPS results and electrophoretic mobility data were used to constrain the fits. While bacteria are inherently complicated, our strategy was to make simplifications that allowed their surface chemistry to be described using a simple model with as few adjustable parameters as possible.

Experimental Section

Reagents. Deionized and boiled water was used to prepare all solutions, and NaCl (Merck, dried overnight at 180 °C) was used to adjust the ionic strength to 0.1 M. Stock solutions of HCl (Fisher p.a.) were standardized against Trizma base (tris(hydroxymethyl)aminomethane). NaOH (Merck p.a.) stock solutions were standardized against standardized HCl solutions.

Bacterial Growth and Freeze-Drying. A *B. subtilis* strain (ATCC code: 6633) was grown at 30 °C in Luria Bertani broth (composition for 1 L of culture medium: yeast extract = 5 g, tryptone = 10 g, NaCl = 5 g) under aerobic conditions on an orbital shaker. The cells were collected by centrifugation at 2880*g* for 20 min at the end of the exponential growth phase, washed twice with physiological solution (NaCl 0.9% by mass), and freeze-dried at −52 °C for 24 h at a pressure of $\sim 10^{-1}$ mbar (Modulyo 4K by Edwards High Vacuum International). Samples for ATR-FTIR spectroscopy, potentiometric titrations, and electrophoretic mobility were prepared by suspending the freeze-dried bacteria in 0.1 M NaCl ionic medium. Images of the freeze-dried bacteria resuspended in ionic medium (0.1 M NaCl) were recorded using a fluorescence microscope (Axiovert 40 CFL Carl Zeiss Microimaging, Inc.) in order to check that the bacterial cells were intact after the freeze-drying procedure.

X-ray Photoelectron Spectroscopy. Freeze-dried samples for XPS were prepared by lyophilizing some bacterial pastes washed with deionized water, and XPS spectra were collected on the dry powders with a Kratos Axis Ultra electron spectrometer using a monochromated Al K_α source operated at 150 W. Analyzer pass energies of 160 and 20 eV were used to acquire the wide spectrum and individual photoelectron lines, respectively. For a more detailed description, see ref *12*.

Attenuated Total Reflection Fourier Transform Infrared (ATR-FTIR) Spectroscopy. ATR-FTIR spectroscopy was used to measure the infrared spectrum of *B. subtilis* as a function of pH. Bacterial suspensions were prepared by resuspending a known amount of freeze-dried bacteria (2.8−3.5 g/L) in 0.1 M NaCl ionic medium. The suspensions were titrated at 25 ± 1 °C using standardized HCl or NaOH prepared in the same ionic medium, and the pH was measured by a combination glass electrode that was calibrated with an acidic solution of known concentration. Aliquots were removed at the desired pH values, and the bacterial cells were collected in the form of wet pastes by centrifugation. An absorbance spectrum was recorded by taking the negative logarithm of the ratio of the single-beam spectrum of the wet paste to the single-beam spectrum of the supernatant solution.

All spectra were collected in a 25 ± 0.2 °C room with a Bruker IFS 66V/S spectrometer equipped with a deuterated triglycine sulfate (DTGS) detector and a silicon carbide water-cooled source. The sample chamber was evacuated to a pressure of 3 mbar to exclude CO_2 and water vapor and for greater temperature stability. A horizontal ATR cell equipped with a nine-reflection diamond crystal was used for the measurements. The angle of incidence was 45° and was far beyond the critical angle. A lid was placed over the sample and pressed against a rubber gasket in order to protect the sample from the vacuum. A total of 300 scans at a resolution of 4 cm^{-1} were averaged over the range 7500 cm^{-1} to 370 cm^{-1}.

Potentiometry. Freeze-dried bacteria were used in the potentiometric titrations to allow quantitative determination of proton uptake by the surface of the cells. Known amounts of freeze-dried bacterial cells were first suspended in an acidic solution (∼50 mM HCl) for 1 h, washed with deionized and boiled water, and finally centrifuged and resuspended in 0.1 M ionic medium. The acid washing procedure was performed in order to remove metal ions and exudates that could be present in the growth medium (*2*, *13*). The OD_{600} of the resulting acid-washed suspension was measured (Spectrophotometer UV-1201 V, Shimadzu), and this value was correlated to the dry weight of the cells, by comparison with a nonacid washed identical suspension of cells in the same ionic medium. The bacterial cells were observed with an optical microscope (KF2 Carl Zeiss, West Germany) after the acid washing procedure in order to ensure that size and shape of the bacteria did not show any changes.

Titrations were performed at 25 ± 0.02 °C using the volumetric method, and the pH was varied by adding aliquots of standardized HCl or NaOH prepared in the same ionic medium. Two titrations were performed in the acidic pH range (from 3.4 to 2.1) and lasted for ∼3 to ∼8 h; two more titrations covered a pH range from 3.4 up to 9.7 and lasted for ∼24 h.

The potential of a glass electrode was measured by means of the cell:

$$\text{GE/BS/RE} \tag{1}$$

where BS indicates the bacterial suspension, GE is the glass electrode and RE is an Ag/AgCl reference electrode placed outside but electrically connected to the solution through a "Wilhelm type" salt bridge. Free proton concentrations were calculated using the Nernst equation:

$$E = E^0 + 59.16 \times \log_{10}[H^+] + E_j \tag{2}$$

where E^0 is the constant of the glass electrode and E_j is the liquid junction potential. A valid expression for E_j is:

$$E_j = j_{ac}[H^+] + j_{alk}K_w[H^+]^{-1} \tag{3}$$

For 0.1 M NaCl, the following values hold (*14*): $j_{ac} = -511$ mV M^{-1}; $j_{alk} = 238.7$ mV M^{-1}; $K_w = 10^{-13.78}$ M^2. The glass electrode constant E^0 was determined by calibrating the electrode in an acidic solution of known proton concentration.

While it is necessary to obtain accurate equilibrated measurements in order to perform thermodynamic modeling, it is also of crucial importance to avoid possible side reactions that a biological system can undergo during acid−base titrations (*15*). For example, it was observed in our experiments that if the bacterial cells were kept for about 9 h at pH values between 8.2 and 9.7, the back-titration with acid was not reversible. This is probably due to bacterial lysis occurring under alkaline conditions and possibly to secretion of exudates from the cells. A certain drift in the potential of the glass electrode (1.4 mV/h at alkaline pH) had to be accepted in order to be able to exclude damage to the bacterial cells (lysis). The titration data that are presented here include

data points which did not exceed drift values of 0.7 mV/h in the acidic pH range (pH 2−4.5), 1.7 mV/h at neutral pH (6.7), and 1.4 mV/h in the alkaline pH range (up to pH 9.7). This means that pH values calculated according to eq 2 did not vary in the last hour by more than 0.01 pH units, 0.03 pH units, and 0.02 pH units in the acidic, neutral, and alkaline ranges, respectively.

Electrophoretic Mobility Measurements. It is reported that the electrophoretic mobility of bacterial suspensions can be used as a qualitative estimate of the bacterial surface charge (*13*). Laser Doppler electrophoretic measurements were performed on a suspension of freeze-dried bacteria in 0.1 M NaCl. Aliquots were removed from the titration vessel during the acid−base potentiometric titration at different pH values (see section potentiometry), and electrophoretic mobilities were measured with a Zetasizer 4 (Malvern Instrument Inc.).

Surface Complexation Modeling. Surface complexation models (*16*, *17*) treat reactions at surfaces using thermodynamic equilibrium expressions corrected for the Coulombic energy of the charged surface. There are several standard electrostatic models used for this correction (*16*), and here we have chosen to apply the simplest, the Constant Capacitance Model (CCM). The CCM has been applied previously to mineral surfaces (*18*), wood fiber surfaces (*19*), and the surface of humic substances (*18*). The measurable stability constant (K) for the protonation of a generic surface functional group ($\equiv SG^n$) with charge n is defined as:

$$K = \frac{[\equiv SGH^{n+1}]}{[\equiv SG^n][H^+]} \quad (4)$$

where $\equiv SGH^{n+1}$ is the protonated form of this functional group, and $[H^+]$ is the proton concentration in the bulk. K is related to the intrinsic stability constant (K^{int}) by:

$$K = K^{int} e^{(-F\psi/RT)} \quad (5)$$

where ψ is the potential at the surface and $e^{(-F\psi/RT)}$ the correction factor that takes into account the build up of surface charge. In the CCM, the electric double layer is modeled as a single parallel-plate capacitor, and the surface potential (ψ) and surface charge density (σ) are related by:

$$\sigma = \kappa\psi \quad (6)$$

where κ is the capacitance. The surface charge density (σ) is defined as:

$$\sigma = T_\sigma F/sa \quad (7)$$

where s is the surface area, a is the solid concentration, and T_σ is the surface charge concentration (*16*).

We used the computer program MAGPIE (*20*) to fit a surface complexation model to our experimental data. MAGPIE minimizes the sum of the squares of the deviations (U) between the calculated and experimental data using a modified Levenberg−Marquardt nonlinear least-squares algorithm where the Jacobian is calculated by a finite difference approach. In the course of the minimization, unknowns are iterated upon until the smallest value of the sum of the squares of the deviations is found. Calculated values are determined using the SGW algorithm by Eriksson (*21*). More details about the MAGPIE software are provided in the Supporting Information.

Results and Discussion

X-ray Photoelectron Spectroscopy. The use of XPS for the study of microbial cell surfaces is well established (*22*). Attempts have been made to correlate spectral information obtained on freeze-dried cells with the properties of bacteria in the hydrated state (*23*). In a previous study, we showed evidence of phosphate ($\equiv PO^-$), carboxylic acid ($\equiv COOH$), and amine ($\equiv NH^+$) surface functional groups from XPS spectra of both freeze-dried and frozen wet pastes of *B. subtilis*. In particular, wet pastes of bacterial cells at different pH values were measured by using a fast freezing procedure of the sample transfer rod, which allowed the study of chemical reactions occurring at the interface between the bacteria and the aqueous solution (*12*). Two components were always present in the N 1s photoelectron line in all the spectra: deprotonated amine or amide moieties ($\equiv N$) at 400.0 eV and protonated amine groups ($\equiv NH^+$) at 401.7 eV. In the fast frozen samples, the ratio of the atomic concentrations (atom %) of $\equiv NH^+$ to $\equiv N$ groups on the surface shows a significant decrease with increasing pH, which is indicative of deprotonation of amine groups. However, it was not possible to determine the protonation states of the carboxylic and phosphate groups, since protonated and nonprotonated surface sites would appear in the XPS spectrum at very close binding energies.

The atomic concentrations (atom %) of the three different surface functional groups were calculated from the P 2p, C 1s, and N 1s spectra of the bacteria as freeze-dried powders. XPS does not allow direct quantitative determination of surface site density in terms of site/nm^2; therefore, the surface atomic concentrations of the phosphate and carboxylic groups were normalized to the amine group content. Three independent replicates were performed, and an average $[\equiv COOH]_{tot}$:$[\equiv NH^+]_{tot}$:$[\equiv PO^-]_{tot}$ ratio of 1.2:1:0.9 was calculated (Table S1, Supporting Information). The accuracy of these results is estimated to be within 10% of their true value. The atomic ratio determined experimentally provides us with an important constraint in determination of the total concentration of the surface sites, as described further in the Modeling section.

ATR-FTIR Spectroscopy. Infrared spectra of wet pastes from suspensions of freeze-dried *B. subtilis* covering pH = 6.5 to pH ∼ 1 were horizontal baseline corrected assuming that the average of the absorbances between 1800 cm^{-1} and 1850 cm^{-1} should be zero. (A two-parameter linear baseline correction could not be used because there were no absorbance values at lower wavenumber that were clearly at the baseline.) An SVD was then performed over the region 915 cm^{-1} to 1825 cm^{-1} in order to determine the number of linearly independent spectra needed to account for the changes as a function of pH (*24*). The results indicated that 99.982% of the variance in the data could be accounted by two basis spectra. The third basis spectrum accounts for only 0.009% of the variance, and the contributions of the second and third basis spectra differ by 2 orders of magnitude. This is a strong indication that only two spectra are required to explain nearly all of the changes in the data. Consistent with our spectral band assignments below, these two spectra are attributed to bacteria with either protonated or deprotonated carboxylate functional groups. While the third basis spectrum accounts for very little of the variance, it is interesting to note that it is dominated by features in the region where the PO stretching modes of phosphate groups absorb (here, from about 950 cm^{-1} to 1275 cm^{-1}). Furthermore, these features are absent if the SVD analysis is performed on only the measured spectra covering the pH range from 6.5 to 2.1. This could be an indication that the phosphate groups are proton active below pH = 2.1.

In order to expose trends in the spectra as a function of pH and to use the spectra directly in our surface complexation modeling, they must be normalized so that they can be related quantitatively to each other. This normalization is required because the distance of the bacteria from the ATR crystal varies with surface charge and thus the effective path length

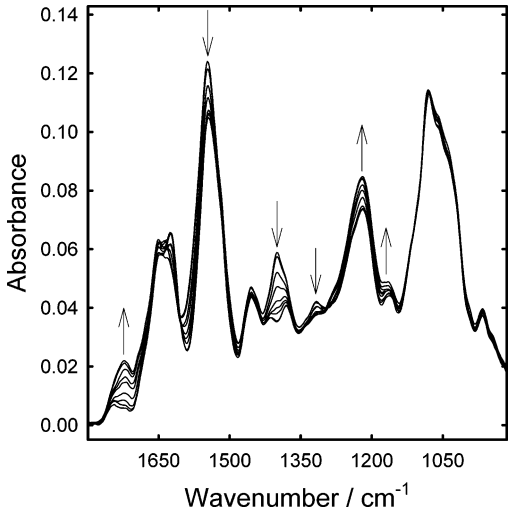

FIGURE 1. 1. ATR-FTIR spectra of wet pastes from suspensions of freeze-dried *B. subtilis* in 0.1 M NaCl ionic medium (∼2.8−3.5 g/L) at the following pH values: 2.1, 2.5, 3.0, 3.5, 3.9, 4.4, 5.0, 5.8, and 6.5. The spectra are horizontal (not linear) baseline corrected by assuming that the average of the absorbances between 1800 cm^{-1} and 1850 cm^{-1} should be zero. They are also normalized by the area under the PO stretching band at 1080 cm^{-1} (see text). The arrows indicate the direction of the change of absorbance with decreasing pH.

through the bacteria changes with pH (*25*). In addition, it is difficult to obtain exactly the same density of the wet paste for each sample. On the basis of the SVD results, we make the approximation that the changes associated with the PO stretching bands are insignificant between pH = 2.1 and pH = 6.5. Thus, we normalize our spectra by assuming that their integrated areas (between 1020 cm^{-1} and 1110 cm^{-1}) under a PO stretching band centered at about 1080 cm^{-1} should be identical. This approach is different from that of previous studies, which used the Amide II band for normalization (*7, 25*).

The baseline corrected and normalized spectra are shown in Figure 1 over the pH range from 2.1 to 6.5 and the fit to the ATR-FTIR spectra is shown in Figure 2. We assign the major bands in these spectra based on the changes observed as a function of pH and in accordance with previous studies (*5, 26*). The peak at 1546 cm^{-1} is traditionally designated as the Amide II band and is assigned to the N−H in plane deformation and, to a lesser extent, the C−N stretching vibrations in amide groups. However, we note that the changes in this band with pH are positively correlated with the band at 1401 cm^{-1}, which is due to the symmetric $-CO_2-$ stretching vibration of carboxylate functional groups. Hence, we also attribute the feature at 1546 cm^{-1} to an asymmetric $-CO_2-$ stretching vibration, which typically absorb between 1540 cm^{-1} and 1640 cm^{-1} in carboxylate-containing molecules (*27*). Similarly, the peak at 1220 cm^{-1} is assigned to a PO stretching band of phosphate groups. However, the changes in this band are positively correlated with the carboxylic acid C═O stretching band at 1722 cm^{-1}. Thus we also assign the peak at 1220 cm^{-1} to the C−OH stretching vibration of carboxylic acid groups.

Electrophoretic Mobility Measurements. The electrophoretic mobility data as a function of pH indicate that the surface of bacterial cells is negatively charged even as low as pH∼1.4 and that the value of the isoelectric point (pH_{iep}) is probably very acidic (between pH ∼ 0.5 and pH ∼ 2), which is in agreement with Fein et al. (*13*) (Figure S1, Supporting Information).

Potentiometric Titrations. The potentiometric titration results from four independent titrations together with the model curve are shown in Figure 3a. The data show good reproducibility. Reversibility was checked in one of these experiments, and these data indicated that the titrations were reversible within our defined equilibration criteria (see Experimental Section). The titration data also show that the pH of immersion is 3.4, and this quite low value suggests that some acidic surface sites are deprotonated as the bacteria are suspended in the ionic medium.

Modeling. Results from XPS and FTIR measurements indicate the presence of carboxylic, phosphate, and amine groups at the surface of *B. subtilis* cells. The phosphate groups are probably in ≡PO^- in phosphodiester structures, which are present in the teichoic and lipoteichoic polymers in the cell wall of Gram-positive bacteria (*28*). Phosphodiester groups typically have pK_a values below 2 (*29−31*), and the presence of these very acidic surface sites is corroborated by the electrophoretic mobility measurements. Amine groups, on the other hand, usually have pK_a values above 7, and carboxylic functional groups typically have pK_a values between 2 and 5 (*29*). The acid washing procedure, described above, probably completely protonated the amine and carboxylate groups, but only a negligible fraction of the phosphate groups. On the basis of this reasoning, we propose the following acid−base equilibria according to the surface complexation modeling formalism (*32*):

$$\equiv COOH \rightleftharpoons \equiv COO^- + H^+ \qquad \beta_{-1,1,0,0} \tag{8}$$

$$\equiv NH^+ \rightleftharpoons \equiv N + H^+ \qquad \beta_{-1,0,1,0} \tag{9}$$

$$\equiv PO^- + H^+ \rightleftharpoons \equiv POH \; \beta_{1,0,0,1} \tag{10}$$

The constants, $\beta_{p,q,r,s}$, are intrinsic formation constants at a surface potential (ψ) of zero in 0.1 M NaCl ionic medium, and *p*, *q*, *r*, and *s* are the stoichiometric coefficients for H^+, ≡COOH, ≡NH^+, and ≡PO^-, respectively. The components ≡COOH, ≡NH^+, and ≡PO^- define the zero level of the total proton concentration $[H^+]_{tot}$:

$$[H^+]_{tot} = [H^+] - [OH^-] - [\equiv COO^-] - [\equiv N] + [\equiv POH] \tag{11}$$

The buildup of surface charge at the cell surface is evident from electrophoretic mobility measurements, and we account for this in our modeling using the constant capacitance model (CCM). This model requires a capacitance (see eq 6), which is an unknown parameter that must be determined from the nonlinear least-squares optimization. The model also requires a value for the bacterial surface area (*s*, see eq 7), and here we use a value of 140 m^2/g estimated previously by Fein et al. (*3*). There is, of course, considerable uncertainty in the estimate of the surface area, especially if one considers the cell wall as a three-dimensional permeable membrane instead of an ion-impenetrable cylindrical surface. However, the capacitance is directly coupled to the surface area (eqs 6 and 7), and therefore an optimized value of the capacitance will account for these uncertainties.

In the absence of any constraints, the computational problem comprises the determination of the capacitance, the intrinsic constants for ≡COOH, ≡NH^+, and ≡PO^-, and the total concentrations of each of the surface sites (a consequence of the absence of pronounced inflection points in the titration curves). This is a total of seven parameters, and we reduce the number of unknowns by using constraints from our spectroscopic results. The fit was *initially* performed under the following conditions (model no. 1):

• The total concentrations were constrained to their 1.2:1:0.9 ratio determined from XPS, removing two unknowns from the computational problem so that only the total concentration of ≡NH^+ groups must be determined. Our

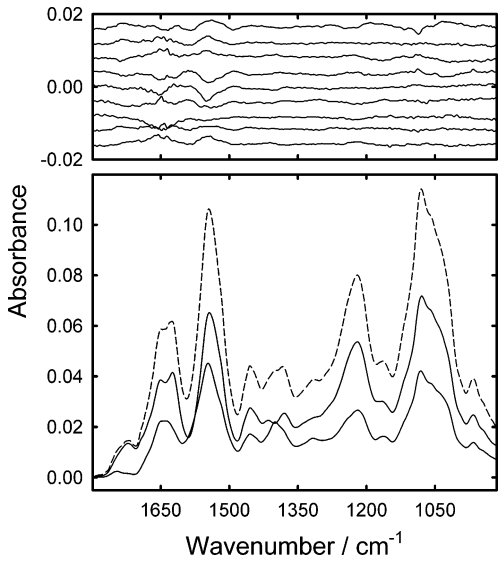

FIGURE 2. 2. (Bottom) An example of the results from a fit to the ATR-FTIR spectrum of a wet paste from a suspension of freeze-dried *B. subtilis* in 0.1 M NaCl (pH = 3.9, ~3.5 g/L suspension) based on model no. 1 (see text and Table 1). The dashed line is the measured spectrum, and the two solid lines are the contributions to the measured spectrum from *B. subtilis* with fully protonated and fully deprotonated carboxylate functional groups. (Top) The residuals from the fits to the measured spectra. The residuals have been offset for clarity, and they are for pH 2.1, 2.5, 3.0, 3.5, 3.9, 4.4, 5.0, 5.8, and 6.5 from bottom to top.

initial guess for this unknown total concentration is based on the total buffer capacity of the system.

• The measured ATR-FTIR spectra are assumed to be a linear combination of only two basis spectra: the spectrum of the bacterium with protonated carboxylate groups, and the spectrum with deprotonated carboxylate groups.

• A total of five unknowns were optimized: the capacitance, the intrinsic deprotonation constants for the ≡COOH, ≡POH, and $\equiv NH^+$ groups, and the total concentration of the $\equiv NH^+$ groups.

Both the ATR-FTIR and potentiometric titration data were fit to this surface complexation model simultaneously. The fit of the model curve to the potentiometric titration data and a corresponding distribution diagram are shown in Figure S2a and S2b (Supporting Information), respectively. The fit to the ATR-FTIR spectra is shown in Figure 2 and the numerical results for this model are reported in Table 1. The fit of the model to the infrared data and to the potentiometric titrations are good, and, in the case of the infrared spectra analysis, this supports the assumptions about normalization and the band assignments discussed above.

Numerical results from the calculations performed by using these constraints include intrinsic stability constants for the carboxylic and amine groups that are in good agreement with the previous work by Fein et al. performed on *B. subtilis* (*13*). However, the capacitance value for our model was an adjustable parameter that was determined in the course of the minimization using the potentiometric and the IR data, and this might explain why it results in disagreement with the same study (*13*). In our model no. 1 we also provide a value for the constant of the phosphodiester groups. However, this value, which is related to the pH_{iep}, is very uncertain considering that potentiometric titration data are only available down to pH ~ 2. Accurate pH measurements are difficult to perform in this very acidic pH range because of the increasing importance of the E_j term in eq 2, and the difference between the large numerical values of the total proton concentration and free proton concentration, $[H^+]_{tot} - [H^+]$ is sensitive to small errors in the measured E values.

It has also been reported (*33*) that acidic conditions alter the structure of the cell wall, which could influence its protonation and surface charge properties.

The value of the intrinsic constant of the phosphodiester groups is calculated to be 2.2, and it results in a conditional pK_a value close to 1.8, as it can be estimated from the distribution diagram (Figure S2b, Supporting Information). The model also predicts a pH_{iep} around 2.9, which is in disagreement with our electrophoretic mobility measurements.

IR data and electrophoretic mobility measurements were performed down to a pH ~ 1 and pH ~ 1.4, respectively, and it is clear that the electrophoretic mobility approaches zero at pH ~ 2. However, from these measurements it is difficult to determine an exact value of the pH_{iep}. IR spectra in this acidic pH range have provided some evidence of protonation of the phosphodiester groups, but quantitative assessment is prevented by significant overlap between the phosphate bands and the strong polysaccharides bands (*34*).

This disagreement between the titration data and electrophoretic mobility data in the acidic pH range was also revealed in the work by Fein et al. on the same type of bacteria (*13*). In our model no. 2 we present one possible solution.

We performed a fit under the same conditions as model no. 1 but with the following modifications:

• We optimized on the total concentrations of *both* the $\equiv NH^+$ and the $\equiv PO^-$ sites. The total concentrations of the ≡COOH and $\equiv NH^+$ sites were constrained to their 1.2:1 ratio determined from XPS.

• The value of the phosphodiester constant ($\log_{10} \beta_{1,0,0,1}$) was manually varied until the minimization led to a model which predicts an pH_{iep} of 1.5.

The fit to the total proton concentration data (Figure 3a) and to the infrared spectra are good. The related distribution diagram is shown in Figure 3b, and the numerical results are reported in Table 1. This model results in a ratio of the total concentrations of $\equiv PO^-$ to $\equiv NH^+$ sites of 1.6:1, which is significantly different from the 0.9:1 ratio reported in Table S1. This deviation between the modeled and measured ratios is justifiable, however. The XPS depth of analysis in the case of organic/biological samples is roughly 10 nm, but the thickness of the cell wall of Gram-positive bacteria, such as *B. subtilis*, can be much greater (~80 nm). Thus, it is possible that a fraction of the teichoic and the lipoteichoic acids, which are the phosphate-containing polymers in the cell wall, is not detected by XPS, but still contributes to the total proton balance and to the surface charge. As suggested in previous works, bacterial surfaces have to be regarded more as heterogeneous polymeric matrixes rather than flat rigid surfaces onto which the surface groups are located. Accordingly, several other models could be used, which would require more parameters for the calculations such as the size and volume of the bacteria and knowledge of the distribution of the functional groups throughout the cell surface.

We have proposed a simple model, which aimed at including as much experimental evidence as possible, both from macroscopic and spectroscopic measurements (infrared spectra and XPS). In particular, XPS data were used here for the first time to our knowledge to constrain the modeling calculations. This is also the first time that IR spectra have been used fully quantitatively in a surface complexation model via a factor analysis. With our simple model, a good agreement with these experimental data is provided.

The model explains the buffering capacity of *B. subtilis* suspensions in a wide pH range (between pH = 3 and pH = 9) which is of considerable environmental interest. In particular, this approach to the modeling of acid−base

TABLE 1. Results of Fits to ATR-FTIR and Potentiometric Titration Data[a]

parameter	reaction	model no. 1[b]	model no. 2[c]
$\log_{10}\beta_{-1,1,0,0}$	$\equiv COOH \rightleftharpoons \equiv COO^- + H^+$	-3.84 ± 0.05	-3.2 ± 0.1
$\log_{10}\beta_{-1,0,1,0}$	$\equiv NH^+ \rightleftharpoons \equiv N + H^+$	-6.1 ± 0.2	-5.5 ± 0.3
$\log_{10}\beta_{1,0,0,1}$	$\equiv PO^- + H^+ \rightleftharpoons \equiv POH$	2.2 ± 0.1	1.3[d]
capacitance (F/m^2)	–	6.6 ± 0.6	6.6 ± 0.6
total concentration $\equiv NH^+$ (mM)[e]	–	2.21 ± 0.04	2.20 ± 0.04
total concentration $\equiv COOH$ (mM)[e]	–	2.63 ± 0.04	2.62 ± 0.04
total concentration $\equiv PO^-$ (mM)[e]	–	2.01 ± 0.04	3.5 ± 0.1

[a] $\beta_{p,q,r,s}$ is the intrinsic formation constant in 0.1 M NaCl ionic medium, and p, q, r, and s are the stoichiometric coefficients for H^+, $\equiv COOH$, $\equiv NH^+$, and $\equiv PO^-$, respectively. Errors are $\pm 1\sigma$ and are uncertainties as determined from the nonlinear least-squares fit. [b] The total concentrations of the $\equiv COOH$, $\equiv NH^+$, and $\equiv PO^-$ sites were constrained to their 1.2:1:0.9 ratio as determined from XPS. [c] The total concentrations of the $\equiv COOH$, $\equiv NH^+$ sites were constrained to a 1.2:1 ratio as determined from XPS. The total concentration of $\equiv PO^-$ was set as an unknown in the fit (see text).[d] This parameter was varied manually in the modeling. [e] 4.2 g/L bacterial suspension.

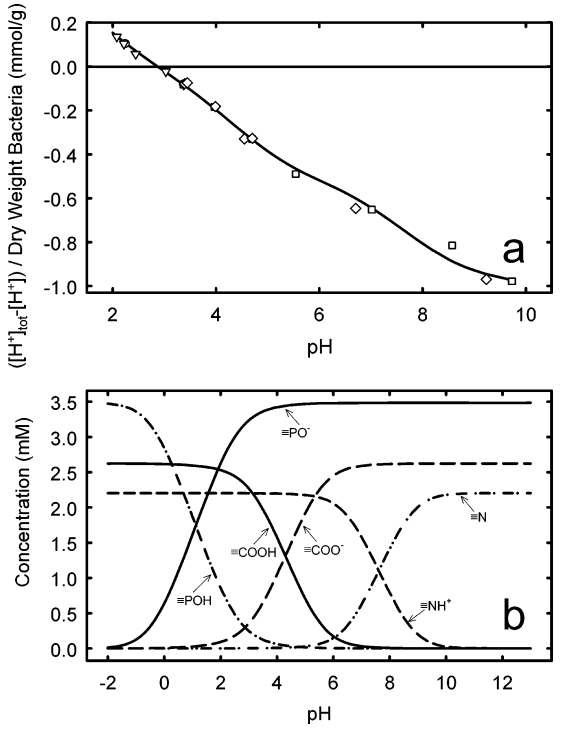

FIGURE 3. 3. (a) The concentration of protons adsorbed ($[H^+]_{tot} - [H^+]$)/dry weight bacteria on the surface of *B. subtilis* in 0.1 M NaCl ionic medium as a function of pH as calculated from the results from four independent potentiometric titrations (indicated using different symbols). The solid line is a fit to the data according to model no. 2, which includes optimizing the total concentration of $\equiv PO^-$ sites (see text and Table 1). (b) Distribution diagram based on model no. 2. (4.2 g/L suspension of *B. subtilis* in 0.1 M NaCl).

properties by combining IR and potentiometric data will open up the possibility of describing other biological surfaces. For example, the protonation constants of the carboxylic groups present on the surface of different types of cultivable bacteria could be similarly determined. Moreover, it is well recognized that in natural samples (for example, soils) the carboxylic groups from the biomass present, the EPS (extracellular polymeric substances), and the humic substances contribute significantly to the acid–base properties. Accordingly, the approach described here may be used to estimate the buffering capacity of organic/biological matter in natural samples.

Acknowledgments

The authors would like to thank Mark Dopson and Olena Rzhepishevska at the Department of Molecular Biology at Umeå University (Sweden) for providing research facilities and supervision regarding the bacterial cultures, Eva Selstam from UPSC (Umeå Plant Science Centre) for her help with the freeze-drying procedure, and Vladimir Zamotin from Medicinal Chemistry and Biophysics Department of Umeå University for helping record images of the bacteria with the fluorescence microscope. This work was supported by the Swedish Research Council. Additional financial contribution by MIUR, the Italian Ministero per l'Istruzione, l'Universita' e la Ricerca, is gratefully acknowledged.

Supporting Information Available

XPS and electrophoretic mobility data, two figures containing results from model no. 1, the values of the sum of the squares of the residuals for both models, and a description of the computer program MAGPIE. This material is available free of charge via the Internet at http://pubs.acs.org.

Literature Cited

(1) McLean, J. S.; Lee, J.-U.; Beveridge, T. J. Interactions of bacteria and environmental metals, fine-grained mineral development and bioremediation strategies. In *Interactions between soil particles and microorganisms, Impact on the terrestrial ecosystem*; IUPAC series on Analytical and Physical Chemistry of Environmental Systems, Volume 8, Huang, P. M., Bollag, J. M., Senesi, N., Eds.; John Wiley and Sons: Chichester, England, 2002.

(2) Daughney, C. J.; Fein, J. B.; Yee, N. A comparison of the thermodynamics of metal adsorption onto two common bacteria. *Chem. Geol.* **1998**, *144*, 161–176.

(3) Fein, J. B.; Daughney, C. J.; Yee, N.; Davis, T. A. A chemical equilibrium model for metal adsorption onto bacterial surfaces. *Geochim. Cosmochim. Acta* **1997**, *61*, 3319–3328.

(4) Stumm, W. *Chemistry of the Solid-Water Interface-Processes at the mineral-water and particle-water interface in natural systems*; John Wiley and Sons: New York, 1992.

(5) Jiang, W.; Saxena, A.; Bongkeun, S.; Bess, B. W.; Beveridge, T. J.; Myneni, S. C. B. Elucidation of functional groups on Gram-positive and Gram-negative bacterial surfaces using infrared spectroscopy. *Langmuir* **2004**, *20*, 11433–11442.

(6) Yee, N.; Benning, L. G.; Phoenix, V. R.; Ferris, G. Characterization of metal-cyanobacteria sorption reactions: a combined macroscopic and infrared spectroscopic investigation. *Environ. Sci. Technol.* **2004**, *38*, 775–782.

(7) Heinrich, H. T. M.; Bremer, P. J.; Daughney, C. J.; McQuillan, J. A. Acid-base titrations of functional groups on the surface of the thermophilic bacterium *Anoxybacillus flavithermus*: comparing a chemical equilibrium model with ATR-IR spectroscopic data. *Langmuir* **2007**, *23*, 2731–2740.

(8) Kelly, S. D.; Kemner, K. M.; Fein, J. B.; Fowle, D. A.; Boyanov, M. I.; Bunker, B. A.; Yee, N. X-ray absorption fine structure determination of pH dependent U-bacterial cell wall interactions. *Geochim. Cosmochim. Acta* **2002**, *66*, 3855–3871.

(9) Boyanov, M. I.; Kelly, K. M.; Kemner, K. M.; Bunker, B. A.; Fein, J. B.; Fowle, D. A. Adsorption of cadmium to *Bacillus subtilis* bacterial cell walls: a pH dependent X-ray absorption fine structure spectroscopy study. *Geochim. Cosmochim. Acta* **2003**, *67*, 3299–3311.

(10) Sarret, G.; Manceau, A.; Spadini, L.; Roux, J. C.; Hazemann, J. L.; Soldo, Y.; Eybert-Berard, L.; Menthonnex, J. J. Structural determination of Zn and Pb binding sites in *Penicillium chrysogenum* walls by EXAFS spectroscopy. *Environ. Sci. Technol.* **1998**, *32*, 1648–1655.

(11) Guiné, V.; Spadini, L.; Sarret, G.; Muris, M.; Delolme, C.; Gaudet, J. P.; Martins, J. M. F. Zinc sorption to three Gram-negative bacteria: combined titration, modeling and EXAFS study. *Environ. Sci. Technol.* **2006**, *40*, 1806−1813.
(12) Leone, L.; Loring, J.; Sjöberg, S.; Persson, P.; Shchukarev, A. Surface characterization of the Gram-positive bacteria *Bacillus subtilis* - an XPS study. *Surf. Interface Anal.* **2006**, *38*, 202−205.
(13) Fein, J. B.; Boily, J. F.; Yee, N.; Gorman-Lewis, D.; Turner, B. F. Potentiometric titrations of *Bacillus subtilis* cells to low pH and a comparison of modeling approaches. *Geochim. Cosmochim. Acta* **2005**, *69*, 1123−1132.
(14) Sjöberg, S.; Hägglund, A.; Nordin, A.; Ingri, N. Equilibrium and structural studies of silicon(IV) and aluminium(III) in aqueous solution. V. Acidity constants of silicic acid and the ionic product of water in the medium range 0.05−2.0 M Na(Cl) at 25 °C. *Mar. Chem*. **1983**, *13*, 35.
(15) Claessens, J.; Behrends, T.; Van Cappellen, P. What do acid-base titrations of live bacteria tell us? A preliminary assessment. *Aquat. Sci.* **2004**, *66*, 19−26.
(16) Lützenkirchen, J.; Boily, J. F.; Sjöberg, S. Current application of and future requirements for surface complexation models. *Curr. Topics Colloid Interface Sci.* **2002**, *5*, 157−190.
(17) Banwart, S. A. Aqueous speciation at the interface between geological solids and groundwater. In *Modelling in aquatic chemistry*; Nuclear Energy Agency: OECD: Paris, 1997.
(18) Nilsson, N. *Inner/outer sphere complexation of phosphate and organic ligands at the goethite-water interface*, Ph.D. thesis, Umeå University, Department of Chemistry, Inorganic Chemistry, 1995.
(19) Lindgren, J. *Experimental studies of the acid-base properties and metal ion affinities of wood fibers*, Ph.D. thesis, Umeå University, Department of Chemistry, Inorganic Chemistry, 2000.
(20) Loring, J. S. MAGPIE, Umeå University, Umeå, Sweden, 2007.
(21) Eriksson, G. An algorithm for the computation of aqueous multi-component, multiphase equilibria. *Anal. Chim. Acta* **1979**, *112*, 375−383.
(22) Van der Mei, H. C.; De Vries, J.; Busscher, H. J. X-ray photoelectron spectroscopy for the study of microbial cell surfaces. *Surf. Sci. Rep.* **2000**, *39*, 1.
(23) Dufrene, Y. F.; Van Der Wal, A.; Norde, W.; Rouxhet, P. G. X-ray photoelectron spectroscopy analysis of whole cells and isolated cell walls of gram-positive bacteria: comparison with biochemical analysis. *J. Bacteriol.* **1997**, *179* (4), 1023.
(24) Malinowski, E. R. *Factor analysis in chemistry*; John Wiley and Sons: New York, 1991.
(25) McWhirter, M. J.; Bremer, P. J.; McQuillan, J. Direct infrared spectroscopic evidence of pH- and ionic strength-induced changes in distance of attached *Pseudomonas aeruginosa* from ZnSe surfaces. *Langmuir* **2002**, *18*, 1904−1907.
(26) Naumann, D.; Schultz, C. P.; Helm, D. What can infrared spectroscopy tell us about the structure and composition of intact bacterial cells? In *Infrared Spectroscopy of Biomolecules*; Mantsch, H. H., Chapman, D., Eds.; John Wiley and Sons: New York, 1996.
(27) Colthup, N. B.; Daly, L. H.; Wiberley, S. E. Chapter 9. In *Introduction to Infrared and Raman Spectroscopy*; Academic Press, Inc.: San Diego, 1990.
(28) Hancock, I. C. Microbial cell surface architecture. In *Microbial Cell Surface Analysis, Structural and Physicochemical Methods*; Mozes, N., Handley, P. S., Busscher, H. J., Rouxhet, P. G., Eds.; VCH Publishers Inc.: New York, 1991.
(29) Martell, A. E.; Smith, R. M. Volume: Other Organic Ligands. In *Critical Stability Constants*; Plenum Press, New York, 1977.
(30) Smith, P. H.; Ekkehardt, H.; Hugi, A.; Raymond, K. N. Crystal structures of two salts of N-(phosphonomethyl)glycine and equilibria with hydrogen and bicarbonate ions. *Inorg. Chem.* **1989**, *28*, 2052.
(31) Lehninger, A. L.; Nelson, D. L.; Cox, M. M. *Principles of Biochemistry*, 2nd ed.; Worth Publishers: New York, 1993.
(32) Stumm, W.; Morgan, J. J. *Aquatic Chemistry*; John Wiley and Sons: New York, 1996.
(33) Borrok, D.; Fein, J. B.; Tischler, M.; O'Loughlin, E.; Meyer, H.; Liss, M.; Kemner, K. M. The effect of acidic solutions and growth conditions on the adsorptive properties of bacterial surfaces. *Chem. Geol.* **2004**, *209*, 107−119.
(34) Heise, H. M. Clinical applications of near and mid-infrared spectroscopy. In *Infrared and Raman Spectroscopy of biological materials*; Gremlich, H.-U., Yan, B., Eds.; Marcel Dekker: New York, 2001; Chapter 8.

Received for review April 27, 2007. Revised manuscript received July 3, 2007. Accepted July 5, 2007.

ES070996E